

## FIELD TESTING OF A WIDEBAND MONITORING CONCEPT AT MV SIDE OF SECONDARY SUBSTATION

Bashir Ahmed SIDDIQUI  
Tampere University of Technology (TUT) – Finland  
bashir.siddiqui@tut.fi

Pertti PAKONEN  
TUT – Finland  
pertti.pakonen@tut.fi

Pekka VERHO  
TUT - Finland  
pekka.verho@tut.fi

### ABSTRACT

Smart grid concept substantially increases the need of monitoring devices in the future for efficient and flexible power delivery. Secondary substation is an ideal location for monitoring both LV and MV networks which can be used to improve the power grid resilience. This paper presents the key features and practical experience gained from the deployment of novel wideband high frequency current transformer (HFCT) sensors for monitoring power quality (PQ) as well as partial discharges (PD) at MV side of the transformer. Additionally, a network simulation is carried out using real-time digital simulator (RTDS) to test the possibility of detecting an earth fault cost-effectively at MV side of secondary substation.

### INTRODUCTION

Distribution network operators are facing considerable network investments in the near future due to the renewal of aging cable networks in cities and renewal of existing underground cables or replacement of overhead lines by underground cables in rural areas. The proliferation of e.g. distributed generation and electronic loads poses new challenges to maintaining the power quality in distribution networks. To focus the network renewals at the correct places in order to decrease the occurrence and duration of unplanned power interruptions and to maintain good power quality proactive network monitoring is becoming essential. Secondary substation is an ideal location to gather large amount of data from LV and MV networks. Secondary substation monitoring would be extremely useful both in MV and LV network fault location and damage assessment and in giving early warnings of incipient faults.

This paper studies the potential of the wideband HFCT sensor which can be installed at MV side of the transformer for partial discharge (PD) monitoring, power quality (PQ) monitoring and disturbance recordings/fault location [1]. HFCT sensors lay the foundation of the novel cost-effective secondary substation monitoring concept presented earlier by the authors [2]. No sensors having expensive high voltage insulations are needed, which makes the solution cost-effective and reliable. In addition, a cost effective way of detecting phase-to-earth faults in the MV network using the HFCT sensors is demonstrated using the RTDS (Real-Time Digital Simulator).

### MAIN FEATURES OF THE WIDEBAND MONITORING CONCEPT

Main features of the wideband monitoring concept are presented in Table 1.  $I_L$ ,  $U_L$ ,  $I_0$  and  $I_n$  refer to MV phase currents, LV phase voltages, MV zero sequence (residual) current and LV neutral current, respectively. The architecture of the wideband monitoring system includes HFCT sensors for current measurements at MV side, resistive divider for voltage measurements at LV side and multichannel data acquisition unit for processing of the data as presented in [2]. However, this paper deals only with the MV-side quantities which depends heavily on the performance of the wideband HFCT sensors.

Table 1. List of monitored quantities at MV and LV side of secondary substation

Quantity	Frequency range		Monitoring function		Channels used			
	HF	LF	Primary	Secondary	PD	PQ	DR	
$I_{L1}$	x	x	PD detection and location	LF: 50 Hz current, current harmonics, transformer loading, cable loading, MV faulty phase detection	x	x	x	
$I_{L2}$	x	x			x	x	x	
$I_{L3}$	x	x			x	x	x	
$I_0$		x	MV fault location				x	
LV-side								
$U_{L1}$	x	x	LV Voltage quality, harmonics, disturbance recording	PD 50 Hz voltage reference, HF: PLC/HF interference, transients, MV phase-to-phase voltages, LV faulty phase detection, fault type assessment	x	x	x	
$U_{L2}$	x	x					x	x
$U_{L3}$	x	x					x	x
$I_n$		x	LV earth fault resistance and location estimation	Neutral conductor loading, neutral conductor fault			x	

HF: frequency range 130 kHz...45 MHz

LF: frequency range 50 Hz...2.5 kHz

### EARTH FAULT LOCATION IN MV NETWORK

An earth fault takes place when one or several phases come in contact with the ground. It is quite common in MV distribution networks where about half of the faults are single-phase earth faults [3]. Early detection of these faults are necessary in order to avoid long outage durations. When an earth fault occurs, initial transient always takes place which has higher amplitude than the steady state fault current and a residual current increase is observed. Traditional protection and control IEDs are unable to detect transients due to high sampling frequency requirements [4].

The principle presented in this paper uses RMS-based detection method. It uses HFCT sensors developed by the authors [1] to measure the three phase currents and the residual current ( $I_0$ ). Such a detection scheme significantly reduces the component costs in the MV network since no voltage measurement is needed.

To describe the detection method, a radial distribution network simulation is performed in the RTDS environment. Figure 1 depicts the single line diagram of the network model used for earth fault detection. The modeled MV network is an isolated neutral network and it consists of four 10 km long underground cable feeders. M2...M4 shows measuring location of three phase currents using HFCT sensors at each secondary substation. M1 is located at MV substation. The fault is assumed to be located near the first secondary substation.

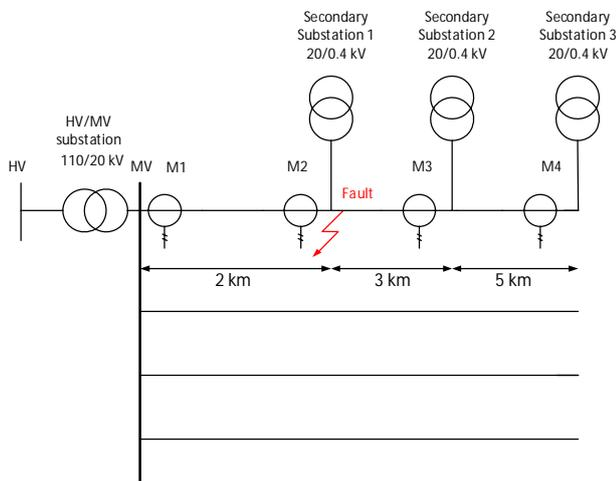


Figure 1. Network model used in RTDS simulation.

Fault is simulated in each phase of the feeder one by one and measured at different locations as indicated by M1...M4. Figure 2 illustrates the case where fault is simulated in phase L1 of the feeder and measured at M1.

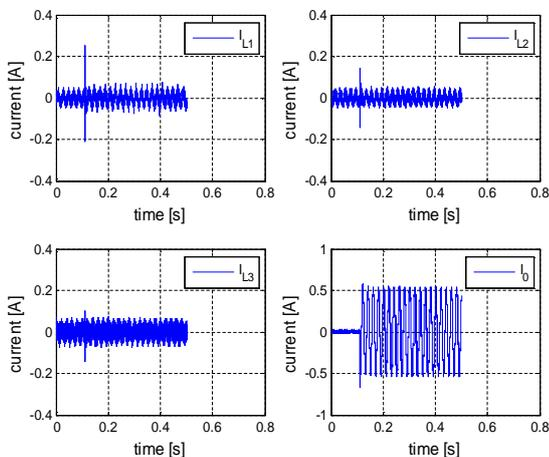


Figure 2. HFCT outputs (phase current derivatives) and residual current measured at M1 in case of fault at L1.

The initial transient phenomenon can be observed in all three phases. During the transient, current flows from one phase to another phase for compensating the change in the network [3]. However, the amplitude of the transient is higher in phase L1 due to the occurrence of the fault in the same phase. Furthermore, residual current ( $I_0$ ) is increased considerably, which is another indication of the earth fault. High frequency noise observed in the phase current derivatives are mainly due to the power electronics of the amplifier and the fact that the HFCT output is a derivative of the phase current (high frequencies are amplified). Numerical integration of the HFCT outputs reduces the noise.

Figure 3 represents the integrated waveforms of the cases where faults occurred in all three phases and measured at M1. A change in the current amplitude of the faulty phase is clearly visible in all cases. A transient is observed in the healthy phases as well but they are quite stable. Due to the earth fault a part of the feeder current returns to the feeding substation via the earth, other feeders and their capacitances to earth which causes the residual current ( $I_0$ ) of the feeder to increase.

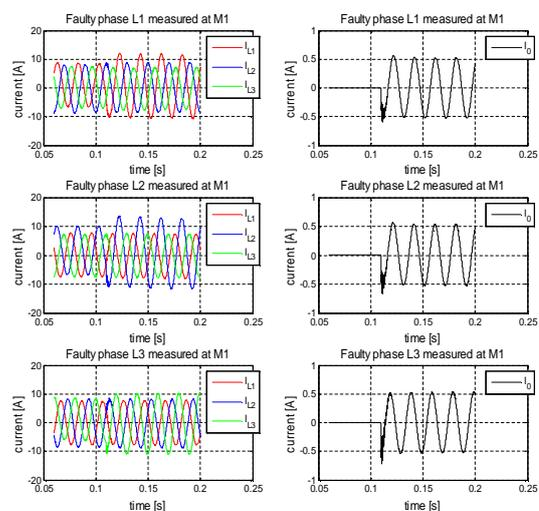


Figure 3. Integrated phase currents and residual currents measured at M1 in case of faults at different phases i.e. L1...L3.

Table 2 depicts detailed analysis of the RMS current of all phases before and after the earth fault measured at location M1. The residual current increases whenever there is a fault in any phase of the feeder. Additionally, RMS current of the respective faulty phase is increasing. Based on the RMS current of the individual feeder, faulty phase of the feeder can be easily identified.

Location of the fault can be estimated based on the proposed concept that the wideband monitor should be installed at each secondary substation [2]. As stated earlier, measurements are performed at different locations i.e. M1...M4 in order to detect the earth fault. For

location estimation, let's use the case with fault in phase L1 only and measurement results from all four locations.

Table 2. RMS current measured by HFCT sensors at M1 before and the after the fault

Fault at L1	RMS currents [A]			
	$I_{L1}$	$I_{L2}$	$I_{L3}$	$I_0$
Before fault	5.59	5.93	5.17	0.0020
After fault	7.88	6.10	5.20	0.37
Fault at L2	RMS currents [A]			
	$I_{L1}$	$I_{L2}$	$I_{L3}$	$I_0$
Before fault	5.37	5.19	5.17	0.0027
After fault	5.42	8.61	5.32	0.37
Fault at L3	RMS currents [A]			
	$I_{L1}$	$I_{L2}$	$I_{L3}$	$I_0$
Before fault	5.38	5.92	5.60	0.0015
After fault	5.54	5.99	7.52	0.37

Table 3 shows the RMS current of the MV feeder with fault in the phase L1 only measured at all four locations. It is noticeable that M1 is located upstream from the fault so the change in the faulty phase current  $I_{L1}$  and  $I_0$  is clearly visible. Since M2 is located upstream of the fault and very close to the fault location, a higher  $I_{L1}$  as well as  $I_0$  can be witnessed. In contrast, measurement from M3 located downstream of the fault does not show significant change in the faulty phase  $I_{L1}$ , whereas  $I_0$  has small change. Similarly, measurement from M4 neither exhibits any change in faulty phase  $I_{L1}$  nor the residual current  $I_0$ . Based on the higher RMS value measured at M2, it can be concluded that the fault is located close to secondary substation 1 upstream of the measurement.

Table 3. Faulty phase L1 currents measured by HFCT sensors before and the after the fault

Location M1	RMS currents [A]			
	$I_{L1}$	$I_{L2}$	$I_{L3}$	$I_0$
Before fault	5.59	5.93	5.17	0.0020
After fault	7.88	6.10	5.20	0.37
Location M2	RMS currents [A]			
	$I_{L1}$	$I_{L2}$	$I_{L3}$	$I_0$
Before fault	5.61	5.96	5.20	0.0027
After fault	7.91	6.10	5.22	0.40
Location M3	RMS currents [A]			
	$I_{L1}$	$I_{L2}$	$I_{L3}$	$I_0$
Before fault	5.42	5.96	5.18	0.0016
After fault	5.24	6.12	5.21	0.10
Location M4	RMS currents [A]			
	$I_{L1}$	$I_{L2}$	$I_{L3}$	$I_0$
Before fault	5.48	6.02	5.24	0.0013
After fault	5.35	6.14	5.25	0.06

Cost-effective implementation of earth-fault detection is challenging. Due to the wideband nature of the HFCT sensor, earth fault detection is possible based on current measurements through retrofit install.

## MV POWER QUALITY MONITORING

The HFCT sensors mainly developed for PD measurements also allow PQ measurement at frequency range below 2.5 kHz at the MV side of the secondary substation. Monitoring the load currents and harmonics on the secondary substations is useful for planning future network investments and e.g. transformer maintenance. Especially, feeders with industrial customers or high penetration of DER can be monitored to extract the information about the harmonic current injection at secondary substation. It would be useful in locating potential causes of power quality problems, assessing the transformer loading and aging [5,6] and the compliance with recommendations given e.g. in IEEE 519 or IEC 61000-3-6 [7,8].

Three HFCT sensors were installed at primary substation around a live 20 kV feeder phase conductors with load current 26 A for PD and PQ measurements. Additionally, a commercial power quality sensor LEM Flex (RR3030) was installed in one of the phases to compare the results. Figure 4 shows time-domain representation of the currents measured at 20 kV feeder by HFCT and the commercial power quality current sensor. Three HFCT sensors were measuring the three consecutive phases of one feeder and LEM was measuring only phase L3. The output of the LEM sensor is clean compared to HFCT outputs because it is already integrated.

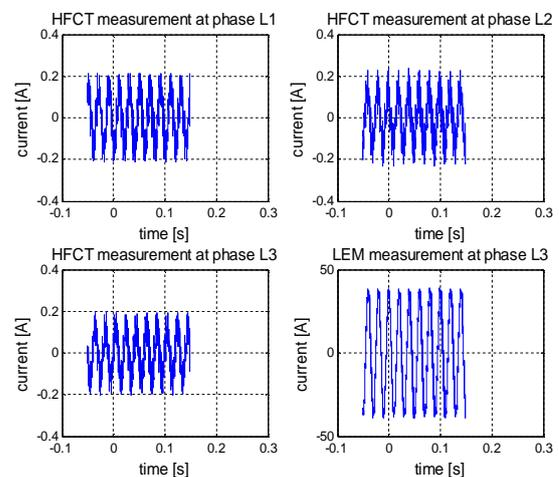


Figure 4. Current measurement at 20 kV feeder using HFCT and LEM current sensors. HFCT waveforms represent the derivatives of the phase currents while LEM waveform is already integrated by the sensor's built in analog integrator.

Let's take a closer look at the output of the HFCT sensor and LEM sensor measured at phase L3 of the feeder. Figure 5 depicts the current measurement of both sensors. HFCT sensor output is also integrated to obtain the actual power frequency current. It is visible that the output produced by HFCT sensor is quite identical to the LEM current sensor output. LEM output is more noise, partly

because of its larger measurement range of up to 300A compared to that of the HFCT (up to 100 A).

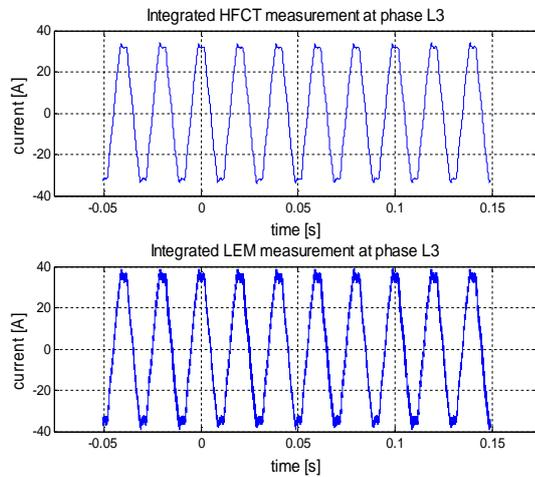


Figure 5. Integrated current waveforms of the HFCT and LEM current sensor measured at phase L3 of the feeder.

In IEC 61000-4-7, 200 ms window is specified for harmonic measurement. Figure 6 represents the frequency-domain analysis of the 200 ms current measured at phase L3 by HFCT and LEM sensor. The fundamental frequency harmonics can be observed in the output of both sensors.

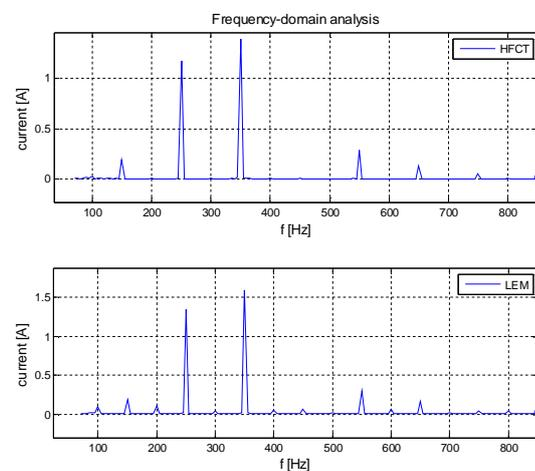


Figure 6. Frequency-domain analysis of the current measured by HFCT and LEM at phase L3 of the feeder.

It can be concluded that the performance of the HFCT sensor is adequate in the field for power quality measurement. It has shown similar results compared with the commercial power quality sensor in terms of the harmonics analysis. Harmonics increase the eddy current losses exponentially causing temperature rise of transformers. Hence, PQ measurements at MV side can help e.g. for estimating thermal loading and hot-spot temperature of the transformer. Moreover, it helps identifying potential power quality problems in the network, which is becoming increasingly important with

the proliferation of distributed generation, electric vehicles and electronic loads.

## PARTIAL DISCHARGE MONITORING

Partial discharge measurement is one of the most versatile tools for detecting incipient faults in transformers, switchgear and underground cables, terminations and joints. HFCT sensors were installed around a live 20 kV feeder phase conductors for PD measurements. The amplitude response of the HFCT sensor is optimized so that by a digital high pass filtering the partial discharges and other high frequency phenomena occurring in the MV network can be monitored with high sensitivity simultaneously with the power frequency current measurement. The HFCT sensors exhibit a flat amplitude response at a frequency range of 130 kHz...45 MHz [1] and as such they are excellent for partial discharge monitoring of underground cable networks. Figure 7 presents the high frequency (HF) information extracted from the measurement data presented in Figure 4 using a digital first order Butterworth high-pass filter having a corner frequency of  $f_c = 25$  kHz. For the sake of clarity, high frequency information is presented here only for three cycles. Due to the high-pass filtering the 50 Hz and harmonic frequencies are absent in channels L1...L3 and high frequency signals can be easily observed. In this case, only very small partial discharge activity can be observed in phase L3.

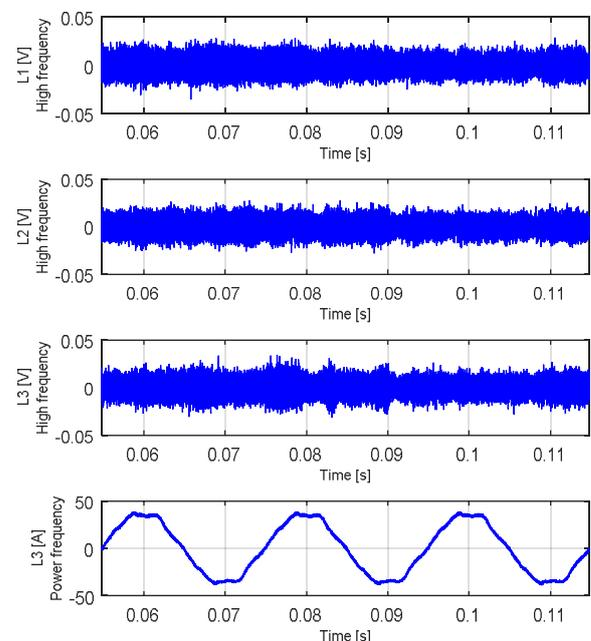


Figure 7. Partial discharge measurement performed at a 20 kV feeder

Figure 8 presents another example of a measurement performed at two 20 kV feeders simultaneously on a 110 / 20 kV primary substation having a double-busbar system. Feeder 1 with a load current of 26 A and feeder 2

with a load current of 80 A were connected to different busbars. In feeder 2, phase L3, high frequency impulses occurring at regular intervals caused by some power electronics device can be observed. The impulses occur at the zero crossings and the commutation notches visible in feeder 2, phase L3, power frequency current waveform presented in the bottom figure. Feeder 1, phases L1 and L3, are almost free of partial discharges and high frequency disturbances.

In conclusion, HFCT sensors have shown promising results in detecting PD and high frequency signals. They can be installed at secondary substation to monitor PD signals on MV cables carrying current up to 100 A over the frequency range of 130 kHz...45 MHz. It also enables the simultaneous recording of the 50 Hz and harmonic current which is a novel approach. The results indicate that using a suitable high-pass filtering partial discharge and high frequency information can be successfully extracted from the raw measurement data containing also power frequency information.

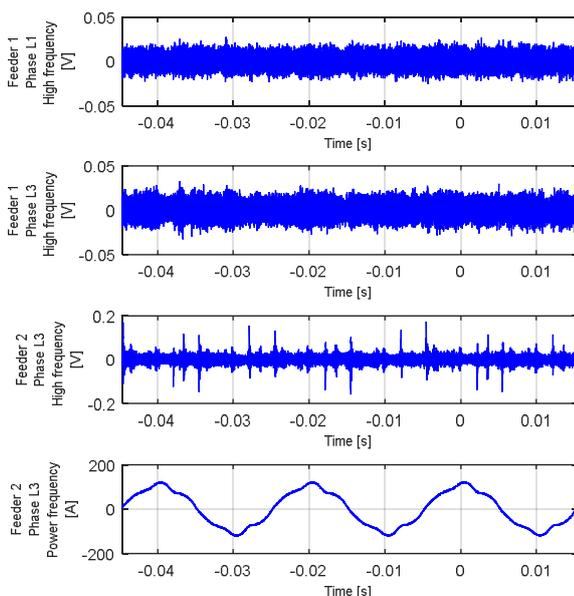


Figure 8. Partial discharge measurement performed at two 20 kV feeders on a 110 / 20 kV primary substation.

## CONCLUSION

Cost-effective wideband high frequency current transformer sensors have been introduced for measurement at MV side of secondary substation. HFCT sensors are the foundation of the novel secondary substation monitoring concept since they reduce the cost of measuring at MV side of the network. A successful testing of the sensors in the field has been carried out for measuring MV-side quantities as shown in Table 1. The performance of the wideband HFCT sensor has fulfilled the expectations considering the fact that they can monitor PQ and PD and locate earth faults. Additionally,

field measurements have proved that HFCT sensors do not experience any saturation when the maximum load current was 80 A.

Future work will concentrate on the development of the data acquisition unit to process the data in real-time. The secondary substation monitoring concept would fundamentally improve the possibilities of predicting and preventing component failures at secondary substations and connected feeders. Information on the voltage level and quality at secondary substations would be useful in network operation (e.g. to increase the hosting capacity of DG) and network planning.

## ACKNOWLEDGMENT

The authors would like to thank the personnel of Tampereen Sähköverkko Oy for offering the possibility to make the field measurements at the substation and for help in the arrangements.

## REFERENCES

- [1] B. A. Siddiqui, P. Pakonen, Pekka Verho, 2017 "Novel Inductive Sensor Solutions for On-line Partial Discharge and Power Quality Monitoring", *IEEE Transactions on Dielectrics and Electrical Insulation*.
- [2] P. Pakonen, B. A. Siddiqui, Pekka Verho, 2016, "A Novel Concept of Secondary Substation Monitoring: Possibilities and Challenges", *IEEE Innovative Smart Grid Technologies (ISGT) Asian 2016 Conference*, Melbourne, Australia, November 2016.
- [3] J. Valtari, 2013, *Centralized Architecture of the Electricity Distribution Substation Automation – Benefits and Possibilities*, Ph.D. Dissertation, Tampere University of Technology, Finland.
- [4] M. Lehtonen, 1992, "Transient Analysis for Ground Fault Distance Estimation in Electrical Distribution Networks", *VTT Technical Research Centre of Finland*, VTT Publications 115.
- [5] J. Fan and S. Borlase, "The evolution of distribution," *IEEE Power and Energy Magazine*, vol. 7, no. 2, pp. 63–68, Mar. 2009.
- [6] R. Godina, et al, 2015, "Effect of Loads and Other Key Factors on Oil-Transformer Ageing: Sustainability Benefits and Challenges", *Energies*, 8, pp. 12147-12186.
- [7] *IEEE Recommended Practices and Requirements for Harmonic Control in Electrical Power Systems*, 1992, ANSI/IEEE Std. 519.
- [8] *Electromagnetic compatibility (EMC)— Part 3–6: Limits — Assessment of emission limits for the connection of distorting installations to MV HV and EHV power systems*, 2008, International Electrotechnical Commission IEC Standard IEC 61000–3–6.